The energy-loss function[16] $-\mathrm{Im}(1/\epsilon)$ of our cubic CdS is also seen in Fig. 4. The peaks of this function correspond to plasma resonances. The peak at 16.4 eV correspond to the plasma resonance of the valence electrons, somewhat modified by the presence of interband transitions originating at the d electrons of the cation. A strong secondary resonance is seen at 11.8 eV. Similar effects have been reported[17] for hexagonal CdS.

The reflection spectrum of the hexagonal CdS deposited on the gallium side of the GaAs substrate shown in Fig. 2 agrees reasonably well with that of bulk hexagonal CdS. In particular, the splitting of E_1 into the $A-B$ doublet and the appearance of the F_1 peak is clearly seen. However, small shifts towards lower energies by about 0.05 eV are seen for the peaks E_0, E_1, E_0', and F_1. These shifts could be due to strains or imperfections. The E_2 peaks seem to have shifted by a larger amount ($\sim$0.2 eV) towards lower energies with respect to those of bulk hexagonal CdS.

Figure 5 shows a section of the reflection spectrum of partially cubic CdS, deposited on the $\{1\bar{1}1\}$ "P face" of GaP, and that of pure hexagonal CdS deposited on the opposite "Ga face." It is seen that the intensity of the A and F_1 peaks is lower for the partially cubic material. Hence a clear indication of the mixed structure of this CdS layer, which is difficult to obtain from x-ray data, is readily obtained from reflectivity measurements. By using the epitaxial deposition technique one should, therefore, be able to obtain optical data for the metastable phases of many III–V, II–VI, and I–VII materials.

[16] H. R. Philipp and H. Ehrenreich, Phys. Rev. **129**, 1550 (1963).

[17] M. Balkanski and Y. Petroff, *Proceedings of the International Conference on the Physics of Semiconductors, Paris 1964* (Dunod Cie, Paris, 1964).

PHYSICAL REVIEW VOLUME 140, NUMBER 2A 18 OCTOBER 1965

Theory of Phonon-Assisted Tunneling in Semiconductors*†

LEONARD KLEINMAN
Department of Physics, University of Southern California, Los Angeles, California
(Received 30 November 1964)

We calculate the phonon-assisted tunneling current for a model p-n junction (as opposed to the homogeneous-electric-field model) due to two mechanisms. A first-order mechanism in which an electron on, say, the p side scatters to a state on the n side with the emission of a phonon yields results similar to those calculated by other workers for the homogeneous-electric-field model and is about three orders of magnitude too small to account for the experimentally observed current. A second-order process in which an electron on the p side tunnels to an intermediate state in a higher band on the n side via the interband term in the Hamiltonian and then scatters with the emission of a phonon to a final state on the n side yields a current equal in magnitude to the experimentally observed current. This mechanism also succeeds, where the first one fails, in accounting for the magnitude of an differences between the experimentally measured pressure coefficients π_{LA}^+, π_{LA}^-, π_{TA}^+, π_{TA}^- where $\pi=J^{-1}dJ/dP$, the superscripts identify the direction of current flow, and the subscripts, the branch of the phonon involved in the tunneling process (LA=longitudinal acoustic, TA=transverse acoustic).

I. INTRODUCTION

THE theory of direct and phonon-assisted indirect tunneling in semiconductors has been developed for the homogeneous-electric-field case by Keldysh[1] and Kane[2] and applied to the heavily doped Esaki[3] p-n junction by Kane.[4] Fredkin and Wannier[5] (hereafter FW) have developed the theory of direct tunneling for a model p-n junction with a constant electric field in the intermediate region and zero field on both the p and n sides. Price and Radcliffe[6] have discussed the p-n junction with position-dependent electric field. FW's work essentially confirms Kane's result. The success of the homogeneous-field model in explaining direct tunneling in p-n junctions is at first sight surprising since in a constant electric field each electron wave function consists of a superposition of all the Bloch functions in the band with a fixed $\mathbf{k}_\perp$, the component of wave vector perpendicular to the electric field. However, it may be understood for the following reasons: (1) Because the tunneling matrix element [Eq. (7) of Ref. 2] depends

* A large portion of this research was accomplished while the author was at the University of Pennsylvania and was there supported by the Advanced Research Projects Agency.

† This work was supported in part by the Joint Services Electronics Programs (U. S. Army, U. S. Navy, and U. S. Air Force) under Contract No. AF-AFOSR-496-64.

[1] L. V. Keldysh, Zh. Eksperim. i Teor. Fiz. **33**, 994 (1957); **34**, 962 (1958) [English transls.: Soviet Phys.—JETP **6**, 763 (1958); **7**, 665 (1958)].

[2] E. O. Kane, J. Phys. Chem. Solids **12**, 181 (1959).

[3] L. Esaki, Phys. Rev. **109**, 603 (1958).

[4] E. O. Kane, J. Appl. Phys. **32**, 83 (1961).

[5] D. R. Fredkin and G. H. Wannier, Phys. Rev. **128**, 2054 (1962).

[6] P. J. Price and J. M. Radcliffe, IBM J. Research Develop. **3**, 364 (1959).

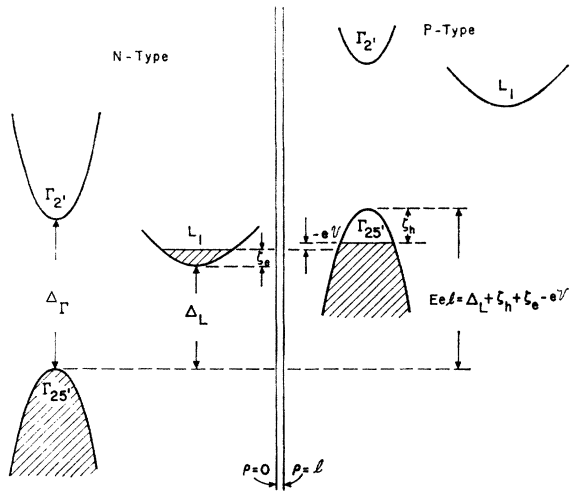

FIG. 1. Energy bands of a model p-n junction with a constant electric field E in the region $0<\rho<l$.

exponentially on the energy difference between the two bands at wave number $\mathbf{k}$, and for *simple* bands this energy difference is stationary only for $k_{11}=0$, tunneling occurs only at $k_{11}=0$ as it does in the FW model. (2) The distance between the turning points of two electrons of the same energy in an electric field E, but in bands separated by a gap Δ, is Δ/eE just as it is in FW's model Esaki diode.

In this paper we develop the theory of phonon-assisted tunneling in the *FW* model p-n junction; we find there are two distinct processes contributing to the phonon-assisted current only one of which has been calculated by Kane[4] for the homogeneous-electric-field case. However, this process yields a current over three orders of magnitude too small to account for the experimentally observed phonon-assisted tunneling current.

Fritzsche and Tiemann[7,8] (hereafter FT[7] and TF[8]) have measured (in Ge) the pressure coefficient of the tunneling current $\pi=J^{-1}dJ/dP$ and found $\pi_{LA}{}^{+}+\pi_{LA}{}^{-}$ to be 50% larger than $\pi_{TA}{}^{+}+\pi_{TA}{}^{-}$, and $\pi_{LA}{}^{-}-\pi_{LA}{}^{+}$ to be four times $\pi_{TA}{}^{-}-\pi_{TA}{}^{+}$, where the superscripts refer to the direction of the current and the subscripts refer to the branch (longitudinal acoustical, transverse acoustical) of the phonon emitted in the tunneling process.[9] They point out that an electron at $\Gamma_{25'}$ in the valence band of the p-type semiconductor may emit a TA phonon (symmetry L_3) and tunnel to the L_1 state in the conduction band of the n-type semiconductor but that the same process involving an LA phonon (symmetry $L_{2'}$) is forbidden on group-theoretical grounds. They quite correctly argue that the LA phonon-assisted tunneling must occur through the intermediate state $\Gamma_{2'}$ (see Fig. 1) ($L_{2'}\times\Gamma_{2'}$ contains L_1 whereas $L_{2'}\times\Gamma_{25'}$ does not) and that this accounts for the differences between π_{LA} and π_{TA}. In TF they argue that in the p-type semiconductor the $\Gamma_{2'}$ level is mixed into the $\Gamma_{25'}$ level through the $\mathbf{k}\cdot\mathbf{p}$ perturbation and then the LA assisted tunneling takes place from $\Gamma_{2'}$ in the p-type semiconductor to L_1 in the n type. They have calculated the TA and LA phonon-assisted currents due to this mechanism and found no substantial forward-reverse asymmetry for either.[10] Furthermore, the magnitude of the current is very close to that obtained by Kane[4] and thus is about three orders of magnitude too small to account for the experimentally observed currents. In FT they describe a completely different mechanism in which a $\Gamma_{25'}$ electron in the p-type semiconductor tunnels to the intermediate $\Gamma_{2'}$ level in the n type through the direct-tunneling interband matrix element and then emits a phonon on scattering to the L_1 state in the n-type semiconductor[11] (see Fig. 1). Their calculation is open to criticism on two counts: (1) Only one intermediate $\Gamma_{2'}$ state is considered rather than a sum over the entire $\Gamma_{2'}$ band. (2) The interband-tunneling matrix element is evaluated by substituting Δ_Γ (the $\Gamma_{25'}-\Gamma_{2'}$ energy gap) for Δ_L (the $\Gamma_{25'}-L_1$ energy gap) in the tunneling matrix element calculated by FW.[5] As we shall show, the FW matrix element has a rather more complicated dependence involving both Δ_Γ and Δ_L which reduces to the simple FW form only when the electron tunnels directly from the valence band of the p-type semiconductor to the conduction band of the n-type (either with or without the emission of a phonon).

In this paper we calculate the first-order TA phonon-assisted current and the second-order LA phonon-assisted current for a model p-n junction. By invoking the $\mathbf{k}\cdot\mathbf{p}$ mixing of $\Gamma_{25'}$ symmetry into the intermediate $\Gamma_{2'}$ states we are also able to estimate the second-order TA phonon-assisted current which would otherwise be forbidden by symmetry. We find that the second-order process of FT accounts well for both the magnitudes and pressure coefficients of the TA and LA currents. Although we have not done it, we think it might be interesting to calculate the second-order phonon-assisted tunneling current for the homogeneous-electric-field case. Because in that case the energy of the intermediate $\Gamma_{2'}$ state is a function of position, there will occur singularities in the energy denominator which Fig. 1 shows cannot occur in the p-n junction. This could conceivably lead to qualitative differences between the two models.

It should be pointed out that our use of the Fredkin-Wannier[5] extended wave functions is quite controversial. There is a school which holds that the electron can be thought of as localized in the semiclassical limit and

[7] H. Fritzsche and J. J. Tiemann (unpublished).

[8] J. J. Tiemann and H. Fritzsche, in *Proceedings of the International Conference on the Physics of Semiconductors, Paris, 1964* (Academic Press Inc., New York, 1965).

[9] π_{TA} is measured in the region of applied voltage $\hbar\omega_{TA}<e\mathcal{V}<\hbar\omega_{LA}$ and π_{LA} in the region $e\mathcal{V}>\hbar\omega_{LA}$ after subtracting off the extrapolated TA-assisted current.

[10] The agreement claimed in Ref. 8 is not correct. H. Fritzsche (private communication).

[11] We will refer to these two processes (TF and FT) as first- and second-order phonon-assisted tunneling.

that WKB considerations are physically meaningful. They picture the electron with a complex $\mathbf{k}$ vector which is a function of the electron's position. At that point in the junction corresponding to a $k_{\parallel}$ which is a branch point in the complex $E(k_{\parallel})$ plane, the electron (in their picture of our second-order process) tunnels into the intermediate (but not virtual) state. A little while later at a position corresponding to a $k_{\parallel}$ which is a point of stationary phase in the electron-phonon matrix element, they picture the electron as tunneling into the final state with the emission of a phonon. In this picture nothing that happens to the electron in the region outside the junction is of consequence; in fact, the calculation is independent of the Fermi levels on the n and p sides. This is to be contrasted with our picture where the scattering of the electron into its final state with the emission of a phonon is *not* a tunneling process and takes place near but not necessarily in the junction.

We would argue with the semiclassical picture on two points. In the first place, in order to get localized electrons it is necessary for the electric field to extend over distances such that $Ed \approx 10$ eV so that a wave packet can be made up of states mixed in from the entire band; this situation does not exist in the p-n junction although it does in the constant-electric-field case. Secondly, even in the constant-field case the semiclassical picture is dangerous to use. Kane in an appendix to his paper[2] has written Ψ (which is made up of a superposition of Bloch states, all from a single band and with real $\mathbf{k}$ vectors) as $\Psi(\mathbf{r},\mathbf{k})$ where $\mathbf{k}$ is itself a function of $\mathbf{r}$. However, he did not use his semiclassical $\Psi(\mathbf{r},\mathbf{k})$ to calculate anything in the body of his paper. Note that if one starts with Ψ a sum of Bloch states in one band, makes the semiclassical approximation but does *not* allow the interband term in the Hamiltonian to perturb Ψ, and then looks at Ψ at a point $\mathbf{k}(\mathbf{r})$ beyond the branch point, Ψ describes an electron in another band! This surprising result appears to be due to the rapidly varying crystal field violating the condition for the validity of the WKB approximation.

II. TUNNELING WAVE FUNCTIONS

In this section we review Sec. V A of FW in order to obtain the wave functions at $\Gamma_{25'}$ in the p-type semiconductor and at L_1 and $\Gamma_{2'}$ in the n-type, as well as the direct $\Gamma_{25'}-\Gamma_{2'}$ tunneling matrix element. We may write the Hamiltonian for the p-n junction in the Wannier representation as $H=H_0+H_1$, with

$$H_0=\omega_n(-i\nabla_\rho)-e\varphi(\rho), \quad H_1=eEX_n, \tag{1}$$

where $\varphi(\rho)$, the potential due to the electric field $E(\rho)$, is taken to be

$$\begin{aligned}\varphi(\rho)&=0, && \rho\leq 0,\\ &=-E\rho, && 0\leq\rho\leq l,\\ &=-El, && \rho\geq l,\end{aligned} \tag{2}$$

and the interband operator X_n operates on eigenfunctions of H_0 as follows:

$$X_n\beta_n=\sum_{n'} X_{nn'}(-i\nabla_\rho)\beta_{n'}, \tag{3}$$

$$X_{nn'}(\mathbf{k})=i\int u_{n\mathbf{k}}^*\frac{\partial}{\partial k}u_{n'\mathbf{k}}d\mathbf{r}, \tag{4}$$

where $u_{n\mathbf{k}}$ is the periodic part of the $\mathbf{k}$th Bloch function in the nth band.

We make the effective-mass approximation for $\omega_n(k)$:

$$\begin{aligned}&\omega_v(\mathbf{k})=-\Delta_L-\hbar^2\mathbf{k}^2/2m_v=-\Delta_L-\mathcal{E}_v^0(\mathbf{k}_v),\\ &\omega_{Lc}(\mathbf{k})=\tfrac{1}{2}\hbar^2\mathbf{k}\cdot(\mathbf{m}_{Lc}^{-1})\cdot\mathbf{k}=\mathcal{E}_{Lc}^0(\mathbf{k}_{Lc}),\\ &\omega_{\Gamma c}(\mathbf{k})=\Delta_\Gamma-\Delta_L+\hbar^2\mathbf{k}^2/2m_{\Gamma c}=\Delta_\Gamma-\Delta_L+\mathcal{E}_{\Gamma c}^0(\mathbf{k}_{\Gamma c}),\end{aligned} \tag{5}$$

where Δ_Γ and Δ_L are the direct and indirect energy gaps shown in Fig. 1, and the subscript v signifies the light-mass $\Gamma_{25'}$ valence band and Γc and Lc the $\Gamma_{2'}$ and L_1 conduction bands. The light-mass valence band is approximated with an isotropic mass, while $\mathbf{m}_{Lc}^{-1}$ is a tensor. Note that we use $\omega_n(\mathbf{k})$ for the energy as measured from the bottom of the L_1 band in the semiconductor of interest, $\mathcal{E}^0(\mathbf{k})$ for the energy as measured from the extremum of the band of interest and later $\mathcal{E}(\mathbf{k})$ for the energy as measured from the bottom of the L_1 band in the n-type semiconductor.

In the region $0<\rho<l$, the Schrödinger equations for $\beta_{\Gamma c}$ and β_{Lc} are

$$[\Delta_\Gamma-\Delta_L+(\hbar^2/2m_{\Gamma c})(\mathbf{k}_\perp^2-d^2/d\rho^2)]\beta_{\Gamma c}+eE\rho\beta_{\Gamma c}=\mathcal{E}_{\Gamma c}, \tag{6}$$

$$\tfrac{1}{2}\hbar^2[\mathbf{k}_\perp\cdot(\mathbf{m}_{Lc}^{-1})\cdot\mathbf{k}_\perp-(m_{Lc}^{-1})_{\parallel}(d^2/d\rho^2)]\beta_{Lc}+eE\rho\beta_{Lc}=\mathcal{E}_{Lc}\beta_{Lc}. \tag{7}$$

Recalling that $\mathcal{E}_{Lc}$ and $\mathcal{E}_{\Gamma c}$ are determined in the n-type region, $\mathcal{E}_{Lc}=\omega_{Lc}(\mathbf{k})$ and $\mathcal{E}_{\Gamma c}=\omega_{\Gamma c}(\mathbf{k})$, defining the classical turning points,

$$\rho_{\Gamma c}=\hbar^2k_{\parallel\Gamma c}^2/2m_{\Gamma c}eE, \quad \rho_{Lc}=\hbar^2k_{\parallel Lc}^2(m_{Lc}^{-1})_{\parallel}/2eE, \tag{8}$$

and making the substitution

$$\xi=\alpha_c(1-\rho/\rho_c), \tag{9}$$

where

$$\alpha_c=(\rho_c k_{\parallel})^{2/3}, \tag{10}$$

we find that Eqs. (6) and (7) both become

$$d^2\beta_c/d\xi^2+\xi\beta_c=0. \tag{11}$$

The solution of (11) which is oscillatory for $\rho<\rho_c$ and decays exponentially for $\rho>\rho_c$ is

$$\beta_c(\rho)=N_cA(\xi)=N_cA[\alpha_c(1-\rho/\rho_c)], \quad 0<\rho<l, \tag{12}$$

where

$$A(x)=\int_{-i\infty}^{i\infty}\exp(\tfrac{1}{3}z^3+xz)dz. \tag{13}$$

We shall need the Fourier transform of $A(x)$,

$$\bar{A}(\kappa)=\int_{-\infty}^{\infty} dx\, e^{-i\kappa x}A(x)=2\pi i\exp(-\tfrac{1}{3}i\kappa^3). \quad (14)$$

In the region $0<\rho\ll\rho_c$, $A(x)$ may be evaluated asymptotically yielding

$$\beta_c(\rho)\sim 2iN_c\pi^{1/2}\alpha_c^{-1/4}(1-\rho/\rho_c)^{-1/4} \times\sin[\tfrac{2}{3}\alpha_c^{3/2}(1-\rho/\rho_c)^{3/2}+\tfrac{1}{4}\pi]. \quad (15)$$

By requiring continuity of amplitude, phase, and derivative of phase, we match (15) to the standing wave outside the junction to obtain

$$\beta_c(\rho)=2iN_c\pi^{1/2}\alpha_c^{-1/4}\sin[-k_{11}\rho+\tfrac{2}{3}\alpha_c^{3/2}+\tfrac{1}{4}\pi], \quad \rho<0. \quad (16)$$

Normalizing the incoming part of $\beta_c(\rho)$ to unity, we obtain

$$N_c=-(V_n\pi)^{-1/2}\alpha_c^{1/4}\exp[i\tfrac{2}{3}\alpha_c^{3/2}+\tfrac{1}{4}\pi], \quad (17)$$

where V_n is the volume of the n side of the junction.

In the region $0<\rho<l$, the Schrödinger equation for β_v is

$$[-\Delta_L-(\hbar^2/2m_v)(k_\perp{}^2-d^2/d\rho^2)]\beta_v+eE\rho\beta_v=\mathcal{E}_v\beta_v. \quad (18)$$

Defining the classical turning point

$$\rho_v=l-\hbar^2k_{11}{}^2/2m_veE, \quad (19)$$

noting that (see Fig. 1.)

$$\mathcal{E}_v=eEl+\omega_v(k)=eEl-\Delta_L-\hbar^2\mathbf{k}^2/2m_v, \quad (20)$$

and substituting

$$\zeta=\alpha_v[1+(\rho-l)/(l-\rho_v)], \quad (21)$$

where

$$\alpha_v=[(-k_{11})(l-\rho_v)]^{2/3}, \quad (22)$$

we find that (18) becomes

$$d^2\beta_v/d\zeta^2+\zeta\beta_v=0, \quad (23)$$

which gives us

$$\beta_v(\rho)=N_vA(\zeta)=N_vA\{\alpha_v[1+(\rho-l)/(l-\rho_v)]\}, \quad 0<\rho<l, \quad (24)$$

where, just as in the calculation of $\beta_c(\rho)$,

$$N_v=(V_p\pi)^{-1/2}\alpha_v^{1/4}\exp[-i(\tfrac{2}{3}\alpha_v^{3/2}+\tfrac{1}{4}\pi)]. \quad (25)$$

III. THE INTERBAND OPERATOR

In this section we derive $X_{vc}(-i\nabla_\rho)$ of Eq. (3) in the four-band model. Kane[12] chooses the z direction to lie along the $\mathbf{k}$ vector and considers the $\mathbf{k}\cdot\mathbf{p}$ perturbation matrix between $\Gamma_{2'}$ and the three fold degenerate $\Gamma_{25'}$. He takes as a basis[13] $|iS\downarrow\rangle$, $|(X-iY)\uparrow/\sqrt{2}\rangle$, $|Z\downarrow\rangle$, $|(X+iY)\uparrow/\sqrt{2}\rangle$, $|iS\uparrow\rangle$, $|-(X+iY)\downarrow/\sqrt{2}\rangle$, $|Z\uparrow\rangle$, $|(X-iY)\downarrow/\sqrt{2}\rangle$, and finds that the 8×8 matrix may be written

$$\begin{vmatrix} H & 0 \\ 0 & H \end{vmatrix},$$

with

$$H=\frac{\hbar^2k^2}{2m}+\begin{vmatrix} \Delta_\Gamma & 0 & kP & 0 \\ 0 & -2\Delta_{S0}/3 & \sqrt{2}\Delta_{S0}/3 & 0 \\ kP & \sqrt{2}\Delta_{S0}/3 & -\Delta_{S0}/3 & 0 \\ 0 & 0 & 0 & 0 \end{vmatrix}, \quad (26)$$

where Δ_{S0} is the spin-orbit splitting of the valence band and

$$P=-i(\hbar/m)\langle S|p_z|Z\rangle. \quad (27)$$

The heavy-hole band in this approximation is not connected to any of the other bands and will henceforth be neglected. If we diagonalize the spin-orbit part of H we find

$$H=\frac{\hbar^2k^2}{2m}+\begin{vmatrix} \Delta_\Gamma & (\frac{2}{3})^{1/2}kP & (\frac{1}{3})^{1/2}kP \\ (\frac{2}{3})^{1/2}kP & 0 & 0 \\ (\frac{1}{3})^{1/2}kP & 0 & -\Delta_{S0} \end{vmatrix}. \quad (28)$$

The spin-orbit splitoff band does not mix with the light-hole band and we treat its admixture into the conduction band by perturbation theory, reducing our four-band model to a two-band model[2]:

$$H=\tfrac{1}{2}\Delta_k+\frac{\hbar^2k^2}{2m}+\begin{pmatrix} \frac{1}{2}\Delta_k & (\frac{2}{3})^{1/2}kP \\ (\frac{2}{3})^{1/2}kP & -\frac{1}{2}\Delta_k \end{pmatrix}, \quad (29)$$

where

$$\Delta_k=\Delta_\Gamma+\tfrac{1}{3}(kP)^2/(\Delta_\Gamma+\Delta_{S0}). \quad (30)$$

The solutions of (29) are

$$E_\pm=\tfrac{1}{2}\Delta_k+\hbar^2k^2/2m\pm\tfrac{1}{2}\eta, \quad (31)$$

$$\eta=(\Delta_k{}^2+8k^2P^2/3)^{1/2}, \quad (32)$$

where $+$ refers to the conduction band Γc, and $-$ to the light-hole valence band v. Using the convention that effective masses are positive quantities, we calculate

$$\frac{\hbar^2}{m_\pm}=\frac{P^2}{3\Delta_\Gamma}\left(4+\frac{\Delta_\Gamma}{\Delta_\Gamma+\Delta_{S0}}\right)\pm\left(\frac{1}{3}\frac{P^2}{\Delta_\Gamma+\Delta_{S0}}+\frac{\hbar^2}{m}\right). \quad (33)$$

Defining a reduced effective mass m_r by

$$m_r{}^{-1}=m_{\Gamma c}{}^{-1}+m_v{}^{-1}, \quad (34)$$

we express P in terms of m_r as follows:

$$P=\hbar\left[3\Delta_\Gamma/2m_r\left(4+\frac{\Delta_\Gamma}{\Delta_\Gamma+\Delta_{S0}}\right)\right]^{1/2}, \quad (35)$$

[12] E. O. Kane, J. Phys. Chem. Solids 1, 249 (1957).

[13] For Ge with a center of inversion make the substitution $X\to YZ$, $Y\to ZX$, $Z\to XY$.

so that (32) becomes, dropping a negligible term in k^4,

$$\eta=(\Delta_\Gamma^2+\Delta_\Gamma\hbar^2k^2m_r^{-1})^{1/2}. \tag{36}$$

The functions $u_{n\mathbf{k}}$ which diagonalize H of Eq. (29) are

$$\begin{aligned} u_{c\mathbf{k}}&=(2\eta)^{-1/2}\{(\eta+\Delta_k)^{1/2}u_{c0}+(\eta-\Delta_k)^{1/2}u_{v0}\},\\ u_{v\mathbf{k}}&=(2\eta)^{-1/2}\{(\eta-\Delta_k)^{1/2}u_{c0}-(\eta+\Delta_k)^{1/2}u_{v0}\}. \end{aligned} \tag{37}$$

Substituting (37) into (4) we find

$$X_{vc}(\mathbf{k})=\frac{i\hbar\Delta_\Gamma^{1/2}}{4m_r^{1/2}}\left[\frac{1}{\Delta_\Gamma+\Delta_{S0}}-\frac{\Delta_k}{\eta^2}\left(4+\frac{\Delta_\Gamma}{\Delta_\Gamma+\Delta_{S0}}\right)\right]\times\left(4+\frac{\Delta_\Gamma}{\Delta_\Gamma+\Delta_{S0}}\right)^{-1/2}. \tag{38}$$

Substituting (30), (35), and (36) into (38) and making a spectral expansion, we write $X_{vc}(-i\nabla_\rho)$ as an integral operator with kernel

$$\begin{aligned} K=-i\left(4+\frac{\Delta_\Gamma}{\Delta_\Gamma+\Delta_{S0}}\right)^{-1/2}\frac{\hbar\Delta_\Gamma^{1/2}}{4m_r^{1/2}}\Bigg\{&\left(4+\frac{\Delta_\Gamma}{\Delta_\Gamma+\Delta_{S0}}\right)\\ &\times\left[\left[1-\frac{\Delta_\Gamma}{\Delta_\Gamma+\Delta_{S0}}\left(8+\frac{2\Delta_\Gamma}{\Delta_\Gamma+\Delta_{S0}}\right)^{-1}\right]\Big/[2\hbar^2m_r^{-1}(\Delta_\Gamma m_r\hbar^{-2}+k_\perp^2)^{1/2}]\right]\\ &\times\exp[-|\rho-\rho'|(\Delta_\Gamma m_r\hbar^{-2}+k_\perp^2)^{1/2}]-(\Delta_\Gamma+\Delta_{S0})^{-1}\delta(\rho-\rho')\Bigg\}. \end{aligned} \tag{39}$$

We could work with the kernel (39), but, for the price of an error considerably smaller than the uncertainties in the four-band model, we greatly simplify (39). Integrating over ρ', we see that when $X_{vc}(-i\nabla_\rho)$ operates on slowly varying functions the delta-function term is about 20% of the exponential term. For the rapidly decaying functions in the tunneling region, however, it is easily shown that the delta function is completely negligible. We make a 2% error by setting $\Delta_\Gamma/(\Delta_\Gamma+\Delta_{S0})$ equal to zero everywhere it appears, to obtain the following kernel:

$$K=-\frac{i}{4}\frac{(\Delta_\Gamma m_r)^{1/2}\exp[-|\rho-\rho'|(\Delta_\Gamma m_r\hbar^{-2}+k_\perp^2)^{1/2}]}{(m_r\Delta_\Gamma+\hbar^2k_\perp^2)^{1/2}}. \tag{40}$$

This is just the kernel one would get from Kane's[2] two-band model; it differs from FW's Eq. (74) because their Eq. (73) for $X_{cv}(\mathbf{k})$ differs from Kane's.

IV. THE INTERBAND MATRIX ELEMENT

In this section we calculate the matrix element of the interband part of the Hamiltonian H_1 by integrating the kernel (40) between the tunneling functions $\beta_{\Gamma c}(\rho)$ and $\beta_v(\rho')$.

$$M(\mathbf{k})=-\tfrac{1}{4}ieE\mathcal{A}\int_{-\infty}^{\infty}\int_{-\infty}^{\infty}\beta_{\Gamma c}(\rho')^*(\Delta_\Gamma m_r)^{1/2}(\Delta_\Gamma m_r+\hbar^2k_\perp^2)^{-1/2}\exp[-|\rho-\rho'|(\Delta_\Gamma m_r\hbar^{-2}+k_\perp^2)^{1/2}]\beta_v(\rho)\,d\rho'\,d\rho, \tag{41}$$

where $\mathcal{A}$ is the area of the junction. Because the integral is negligible outside the region $0<\rho<l$ we have been able to extend the region of ρ integration to $\pm\infty$. For the same reason we may use Eqs. (12) and (24) (which are valid only in the region $0<\rho<l$) for $\beta_{\Gamma c}$ and β_v. Expressing $\beta_{\Gamma c}$ and β_v as Fourier integrals we obtain

$$\begin{aligned} M(\mathbf{k})=\tfrac{1}{4}ieE\mathcal{A}N_{\Gamma c}^*N_v(2\pi)^{-2}&\left[\frac{\rho_{\Gamma c}}{\alpha_{\Gamma c}}\frac{(\rho_v-l)}{\alpha_v}\right]\frac{(\Delta_\Gamma m_r)^{1/2}}{(\Delta_\Gamma m_r+\hbar^2k_\perp^2)^{1/2}}\\ &\times\int\int_{-\infty}^{\infty}\int d\kappa'\,d\kappa\,d\rho'\,d\rho\,\tilde{A}\left(\frac{l-\rho_v}{\alpha_v}\kappa\right)\tilde{A}^*\left(-\frac{\rho_{\Gamma c}}{\alpha_{\Gamma c}}\kappa'\right)\\ &\times\exp[i(\kappa\rho-\kappa'\rho'+\kappa'\rho_{\Gamma c}-\kappa\rho_v)-|\rho-\rho'|(\Delta_\Gamma m_r\hbar^{-2}+k_\perp^2)^{1/2}]. \end{aligned} \tag{42}$$

On integration over the variables $(\rho-\rho')$, ρ', and κ', (42) becomes

$$\begin{aligned} M(\mathbf{k})=ieE(4\pi\hbar)^{-1}\mathcal{A}N_{\Gamma c}^*N_v&\left[\frac{\rho_{\Gamma c}}{\alpha_{\Gamma c}}\frac{(\rho_v-l)}{\alpha_v}\right](\Delta_\Gamma m_r)^{1/2}\\ &\times\int_{-\infty}^{\infty}d\kappa\tilde{A}\left(\frac{l-\rho_v}{\alpha_v}\kappa\right)\tilde{A}^*\left(\frac{-\rho_{\Gamma c}}{\alpha_{\Gamma c}}\kappa\right)(\kappa^2+\Delta_\Gamma m_r\hbar^{-2}+k_\perp^2)^{-1}e^{i(\rho_{\Gamma c}-\rho_v)\kappa}. \end{aligned} \tag{43}$$

Through substitution from Eq. (14) the integral in (43) becomes

$$I=-(2\pi)^2\int_{-\infty}^{\infty}d\kappa(\kappa^2+\Delta_\Gamma m_r\hbar^{-2}+k_\perp^2)^{-1}\exp\left[i(\rho_{\Gamma c}-\rho_v)\kappa-\tfrac{1}{3}i\left(\frac{l-\rho_v}{\alpha_v}\kappa\right)^3-\tfrac{1}{3}i\left(\frac{\rho_{\Gamma c}}{\alpha_{\Gamma c}}\kappa\right)^3\right]$$

$$=-(2\pi)^2\int_{-\infty}^{\infty}d\kappa(\kappa^2+\Delta_\Gamma m_r\hbar^{-2}+k_\perp^2)^{-1}\exp[i(eE)^{-1}\{(\tfrac{1}{2}\hbar^2k_{\|\Gamma c}{}^2m_{\Gamma c}{}^{-1}+\tfrac{1}{2}\hbar^2k_{\|v}{}^2m_v{}^{-1}-eEl)\kappa-\tfrac{1}{6}\hbar^2m_r{}^{-1}\kappa^3\}], \quad (44)$$

where we have used (8), (10), (19), and (22). Note that the term linear in κ in the exponential cannot be simplified to depend only on the energy gap as it can be for direct tunneling.[14] We may perform the integration by the method of steepest descents if we deform the path of integration through the saddle point at $\kappa_s=-i[2m_r\hbar^{-2}(eEl-\frac{1}{2}\hbar^2k_{\|\Gamma c}{}^2m_{\Gamma c}{}^{-1}-\frac{1}{2}\hbar^2k_{\|v}{}^2m_v{}^{-1})]^{1/2}\sim-i(2m_r\hbar^{-2}\Delta_L)^{1/2}$. However in deforming the path of integration we pick up a contribution from the pole at $\kappa_p=-i(\Delta_\Gamma m_r\hbar^{-2}+k_\perp{}^2)^{1/2}\sim-i(\Delta_\Gamma m_r\hbar^{-2})^{1/2}$. As long as $2\Delta_L$ is sufficiently greater than Δ_Γ (as is the case for Ge) the contributon from the pole is exponentially larger than the saddle-point contribution and is the only one we will consider. Thus, by the method of residues,

$$I=4\pi^3(\Delta_\Gamma m_r\hbar^{-2}+k_{\perp v}{}^2)^{-1/2}\exp[-(eE)^{-1}(\Delta_\Gamma m_r\hbar^{-2}+k_{\perp v}{}^2)^{1/2}$$
$$\times\{(eEl-\tfrac{1}{2}\hbar^2k_{\|\Gamma c}{}^2m_{\Gamma c}{}^{-1}-\tfrac{1}{2}\hbar^2k_{\|v}{}^2m_v{}^{-1})-\tfrac{1}{6}(\Delta_\Gamma+\hbar^2k_{\perp v}{}^2m_r{}^{-1})\}], \quad (45)$$

so that

$$M(\mathbf{k})=\hbar^2\left(\frac{k_{\|\Gamma c}(-k_{\|v})}{m_vm_{\Gamma c}}\right)^{1/2}\frac{\pi}{2L}\left(\frac{\Delta_\Gamma m_r}{\Delta_\Gamma m_r+\hbar^2k_{\Gamma v}{}^2}\right)^{1/2}\exp[\tfrac{1}{3}i\hbar^2(eE)^{-1}(k_{\|v}{}^3m_v{}^{-1}-k_{\|\Gamma c}{}^3m_{\Gamma c}{}^{-1})]$$
$$\times\exp[-(eE)^{-1}(\Delta_\Gamma m_r\hbar^{-2}+k_{\perp v}{}^2)^{1/2}(Eel-\tfrac{1}{2}\hbar^2k_{\|\Gamma c}{}^2m_{\Gamma c}{}^{-1}-\tfrac{1}{2}\hbar^2k_{\|v}{}^2m_v{}^{-1}-\tfrac{1}{6}\Delta_\Gamma-\tfrac{1}{6}\hbar^2k_{\perp v}{}^2m_r{}^{-1})], \quad (46)$$

where

$$L=(V_pV_n)^{1/2}/\mathcal{A}.$$

At this point some justification of the use of the effective mass β's instead of the exact β's obtained by substituting (31) in (1) should be made. One might worry that because the pole in (44) is also a branch point of (31), the use of the exact β's in (41) would yield a result different in structure from (46). In the direct-tunneling problem Fredkin and Wannier[5] made exactly the same approximation and obtained a result differing from Kane's[2] by only the numerical factor 1.06. The effect of using the exact β's on the integrand of (44) would be to make $m_{\Gamma c}$ and m_v^{-1} functions of κ. Remembering that κ is real and that most of the integral comes from the region of small κ, we see that the effective-mass approximation (constant $m_{\Gamma c}$ and m_v) is quite good. That we choose to evaluate (44) by integrating in the complex κ plane can have no effect on the validity of the approximation we made to obtain (44). The same comment will apply to Eqs. (50) and (60) where integrals over real wave numbers are again evaluated by saddle-point methods.

V. FIRST-ORDER TA PHONON-ASSISTED TUNNELING

The wave functions for the $\Gamma_{25'}$ light mass and L_1 bands in the tunneling region may be written in the form

$$\psi(\mathbf{k},\mathbf{r})=e^{i\mathbf{k}_\perp\cdot\mathbf{r}}\beta(\rho)u(\mathbf{k},\mathbf{r}), \quad (47)$$

where $\beta(\rho)$ is the apporpriate solution of the Wannier equation of Sec. II and $u(\mathbf{k},\mathbf{r})$ is the periodic part of the Block function whose $\mathbf{k}$ vector is given by its value outside the tunneling region.

We calculate the first-order TA phonon-assisted tunneling current (assuming a temperature sufficiently low that only phonon-emission processes are important) by applying the golden rule:

$$J=(2\pi e/\hbar)\sum_{\mathbf{k}_{\Gamma c}}\sum_{\mathbf{k}_v}\sum_{\text{phonon}}|\langle\psi_{Lc}(\mathbf{k}_{Lc})|H_{\text{TA el ph}}|\psi_v(\mathbf{k}_v)\rangle|^2(f_{Lc}-f_v)\delta(\mathcal{E}_{Lc}-\mathcal{E}_v\mp\hbar\omega), \quad (48)$$

where the $-(+)$ sign holds for positive (negative) applied voltage, i.e., for tunneling from the n (p) side to the p (n) side, and the $f_{c,v}$ are Fermi functions. Although both β_{Lc} and β_v decay quite rapidly in the tunneling region, their product is much more nearly constant so that

$$\langle\psi_{Lc}(\mathbf{k}_{Lc})|H_{\text{TA el ph}}|\psi_v(\mathbf{k}_v)\rangle\approx M_{\text{TA}}V_{\text{ph}}{}^{-1/2}\langle\beta_{Lc}(k_{\|c})|\beta_v(k_{\|v})\rangle, \quad (49)$$

where $M_{\text{TA}}V_{\text{ph}}{}^{-1/2}$ is the TA phonon matrix element between $\Gamma_{25'}$ and L_1 Bloch functions and V_{ph} is the normaliza-

[14] In that case $\hbar^2k_{\|c}{}^2/2m_c=\omega_c-\hbar^2\mathbf{k}_\perp{}^2/2m_c=\mathcal{E}_c-\hbar^2\mathbf{k}_\perp{}^2/2m_c$ and $\hbar^2k_{\|v}{}^2/2m_c=-\Delta-\omega_v-\hbar^2\mathbf{k}_\perp{}^2/2m_v=-\Delta+eEl-\mathcal{E}_v-\hbar^2\mathbf{k}_\perp{}^2/2m_r$. Adding these two terms to $-eEl$, using conservation of energy, i.e., $\mathcal{E}_c=\mathcal{E}_v$, and conservation of $\mathbf{k}_\perp$, we obtain $-i(eE)^{-1}(\Delta+\hbar^2\mathbf{k}_\perp{}^2/2m_r)$ for the coefficient of κ.

tion volume. We proceed to calculate

$$\langle\beta_{Lc}|\beta_v\rangle=\mathfrak{A}N_{Lc}^*N_v\int_0^l d\rho\, A^*[\alpha_{Lc}(1-\rho/\rho_{Lc})]A\left[\alpha_v\left(1+\frac{\rho-l}{l-\rho_v}\right)\right],$$

$$\approx\mathfrak{A}N_c^*N_v\frac{\rho_{Lc}}{\alpha_{Lc}}\frac{\rho_v-l}{\alpha_v}\int_{-\infty}^{\infty}d\kappa\frac{d\kappa'}{(2\pi)^2}d\rho\tilde{A}\left(\frac{l-\rho_v}{\alpha_v}\kappa\right)\tilde{A}^*\left(-\frac{\rho_{Lc}}{\alpha_{Lc}}\kappa'\right)$$

$$\times e^{i(\kappa-\kappa')\rho}e^{i(\kappa'\rho_{Lc}-\kappa\rho_v)}=\mathfrak{A}N_c^*N_v\frac{\rho_{Lc}}{\alpha_{Lc}}\frac{\rho_v-l}{\alpha_v}2\pi\int_{-\infty}^{\infty}d\kappa e^{i(\rho_{Lc}-\rho_v)\kappa}e^{-i\hbar^2\kappa^3/6eEm_{Lr}},\quad(50)$$

where $\mathfrak{A}$ is the area of the junction and $m_{Lr}^{-1}=m_v^{-1}+(m_{Lc}^{-1})_{11}$. A straightforward saddle-point integration yields

$$\langle\beta_{Lc}|\beta_v\rangle=(2\pi)^{3/2}\mathfrak{A}\frac{\rho_{Lc}}{\alpha_{Lc}}\frac{\rho_v-l}{\alpha_v}N_{Lc}^*N_v\left[\frac{eEm_{Lr}}{2\hbar^2(\rho_v-\rho_{Lc})}\right]^{1/4}\exp\{-\tfrac{2}{3}\hbar^{-1}[2eE(\rho_v-\rho_{Lc})^3m_{Lr}]^{1/2}\}$$

$$=\frac{2\hbar^2}{LeE}\left(\frac{eEm_{Lr}}{2\hbar^2(\rho_v-\rho_{Lc})}\right)^{1/4}[\pi k_{11Lc}(-k_{11v})(m_{Lc}^{-1})_{11}/2m_v]^{1/2}\exp\{-\tfrac{2}{3}\hbar^{-1}[2eE(\rho_v-\rho_{Lc})^3m_{Lr}]^{1/2}\},\quad(51)$$

where we have dropped unimportant phase factors from $N_c^*N_v$ and (see Ref. 14)

$$\rho_{Lc}-\rho_v=(eE)^{-1}(-\mathcal{E}_{1v}^0-\mathcal{E}_{1Lc}^0+\mathcal{E}_{Lc}-\mathcal{E}_v-\Delta_L).\quad(52)$$

Substituting (49), (51), and (52) into (48), we may drop the sum over phonons because $M_{\mathrm{TA}}^2V_{\mathrm{ph}}^{-1}$ implicitly contains a δ function of wave vector if V_{ph} is taken to be the volume in which the electron-phonon interactions of interest may take place, $V_{\mathrm{ph}}=(\rho_v-\rho_{Lc})\mathfrak{A}$, rather than the volume of the entire $p-n$ junction.[15] We change the sum over $\mathbf{k}_{Lc}$ and $\mathbf{k}_v$ to integrals over $V(2\pi)^{-3}d^3k$ and use

$$k_{11}d^3k=k_{11}dk_{11}d^2k_1=[\hbar^4(m^{-1})_{11}(m^{-1})_1]^{-1}d\mathcal{E}_{11}^0d\mathcal{E}_1^0d\theta=[\hbar^4(m^{-1})_{11}(m^{-1})_1]^{-1}d\mathcal{E}^0d\mathcal{E}_1^0d\theta,\quad(53)$$

[where $(m^{-1})_1$ is the geometric average of the maximum and minimum values of $\mathbf{k}_1\cdot(\mathbf{m}^{-1})\cdot\mathbf{k}_1/\mathbf{k}_1^2$] to obtain

$$J=\frac{2\sqrt{2}e}{\hbar^6(2\pi)^2}M_{TA}{}^2\mathfrak{A}\frac{m_vm_{Lr}{}^{1/2}}{(m_{Lc}^{-1})_1}\int_0^\infty\int_0^\infty\int_0^{\mathcal{E}_v{}^0}\int_0^{\mathcal{E}_{Lc}}(f_{Lc}-f_v)(\mathcal{E}_{1v}{}^0+\mathcal{E}_{1Lc}{}^0-\mathcal{E}_{Lc}+\mathcal{E}_v+\Delta_L)^{-3/2}$$

$$\times\exp[-\tfrac{4}{3}(2m_{Lr})^{1/2}(eE\hbar)^{-1}(\mathcal{E}_{1v}{}^0+\mathcal{E}_{1Lc}{}^0-\mathcal{E}_{Lc}+\mathcal{E}_v+\Delta_L)^{3/2}]\delta(\mathcal{E}_{Lc}-\mathcal{E}_v\mp\hbar\omega)d\mathcal{E}_{1Lc}{}^0d\mathcal{E}_{1v}{}^0d\mathcal{E}_{Lc}{}^0d\mathcal{E}_v{}^0.\quad(54)$$

We expand the exponential to $\exp[-\frac{4}{3}(2m_{Lr})^{1/2}(eE\hbar)^{-1}\{(\mathcal{E}_v-\mathcal{E}_{Lc}+\Delta_L)^{3/2}+\frac{3}{2}(\mathcal{E}_v-\mathcal{E}_{Lc}+\Delta_L)^{1/2}(\mathcal{E}_{1v}{}^0+\mathcal{E}_{1Lc}{}^0)\}]$, ignore $\mathcal{E}_1{}^0$ where it appears outside the exponential and integrate over $\mathcal{E}_{1Lc}{}^0$, $\mathcal{E}_{1v}{}^0$, and $\mathcal{E}_v{}^0$ using Eq. (20) to obtain

$$J=\frac{\sqrt{2}\mathfrak{A}eM_{\mathrm{TA}}{}^2(eE)^2m_v\exp[-\frac{4}{3}(2m_{Lr})^{1/2}(eE\hbar)^{-1}(\Delta_L\mp\hbar\omega)^{3/2}]}{4(2\pi)^2m_{Lr}{}^{1/2}\hbar^4(m_{Lc}^{-1})_1(\Delta_L\mp\hbar\omega)^{5/2}}$$

$$\times\int_0^\infty d\mathcal{E}_{Lc}(f_{Lc}-f_v)\{1-\exp[-2(2m_{Lr})^{1/2}(eE\hbar)^{-1}(\Delta_L\mp\hbar\omega)^{1/2}(\zeta_h+\zeta_e-e\mathcal{V}-\mathcal{E}_{Lc}\pm\hbar\omega)]\}$$

$$\times\{1-\exp[-2(2m_{Lr})^{1/2}(eE\hbar)^{-1}(\Delta_L\mp\hbar\omega)^{1/2}\mathcal{E}_{Lc}]\}.\quad(55)$$

For the values of ζ_e and ζ_h given by Fritzsche and Tiemann,[16] the exponentials in the integral are not negligible as sometimes is assumed. At the temperature (4°K) at which the experiments are done, the Fermi functions may be replaced by step functions and the integral done between the limits given in Table I. In Sec. VII, we evaluate the integral in the low-voltage range and find the current to be two orders of magnitude smaller than experiment. The same first-order process applied to the LA-assisted case yields a current three orders of magnitude too small. (The experimental LA current is four times larger than the TA while theoretically it is only half as big because of the two TA branches.)

VI. SECOND-ORDER LA PHONON-ASSISTED TUNNELING

In this section we calculate the current due to the following processes. With negative applied voltage an

[15] This may be seen as follows: The product $\beta_{Lc}(k_{11c})\beta_v(k_{11v})$ may be written as a periodic function times $\Sigma A_{\delta k11}\exp[(k_{11c}-k_{11v}-\delta k_{11})\rho]$, where $A_{\delta k11}=\int\beta_{Lc}^*(k_{11c})\beta_v(k_{11v})e^{i\delta k11\rho}d\rho$ and Eq. (51) gives $A_{\delta k11}$ for $\delta k_{11}=0$. If the crystal is N atoms thick then there are Ndi fferent δk_{11}'s; however, the number of δk_{11}'s for which $A_{\delta k11}\approx A_{\delta k11=0}$ is given by $V_{x\ \mathrm{tal}}/(\rho_v-\rho_{Lc})\mathfrak{A}$. Thus $M_{\mathrm{TA}}{}^2V_{x\ \mathrm{tal}}{}^{-1}$ times the number of phonons contributing appreciably to the sum in Eq. (48) is just $M_{\mathrm{TA}}{}^2V_{\mathrm{ph}}{}^{-1}$.

[16] H. Fritzsche and J. J. Tiemann, Phys. Rev. **130**, 617 (1963).

TABLE I. Limits of integration in current integrals (55) and (66) when Fermi functions are replaced by step functions. The following relation holds between $\mathcal{E}_v^0$ and $\mathcal{E}_{Lc}=\mathcal{E}_{Lc}^0$: $\mathcal{E}_v^0=\zeta_h+\zeta_e-e\mathcal{V}\pm\hbar\omega-\mathcal{E}_c$ where the upper (lower) sign holds for positive (negative) voltage. This table is valid only when $\zeta_h>\zeta_e$.

Range of $e\mathcal{V}$	Lower limit of $\mathcal{E}_{Lc}$	Upper limit of $\mathcal{E}_{Lc}$	Lower limit of $\mathcal{E}_v^0$	Upperl imit of $\mathcal{E}_v^0$
$e\mathcal{V}<0$	$\zeta_e-e\mathcal{V}-\hbar\omega$	ζ_e	$\zeta_h-e\mathcal{V}-\hbar\omega$	ζ_h
$0<e\mathcal{V}<\zeta_e+\hbar\omega$	$\zeta_e-e\mathcal{V}+\hbar\omega$	ζ_e	$\zeta_h-e\mathcal{V}+\hbar\omega$	ζ_h
$\zeta_e+\hbar\omega<e\mathcal{V}<\zeta_h+\hbar\omega$	0	ζ_e	$\zeta_h-e\mathcal{V}+\hbar\omega$	$\zeta_h+\zeta_e-e\mathcal{V}+\hbar\omega$
$\zeta_h+\hbar\omega<e\mathcal{V}<\zeta_e+\zeta_h+\hbar\omega$	0	$\zeta_e+\zeta_h-e\mathcal{V}+\hbar\omega$	0	$\zeta_h+\zeta_e-e\mathcal{V}+\hbar\omega$

electron tunnels from a $\Gamma_{25'}$ state on the p side to a virtual state in the $\Gamma_{2'}$ band on the n side via H_1, the interband part of the Hamiltonian, and then scatters to an L_1 state on the n side with the emission of a phonon. With positive applied voltage an L_1 electron on the n side emits a phonon on scattering to a virtual state in the $\Gamma_{2'}$ band on the same side and then tunnels via H_1 to a $\Gamma_{25'}$ state on the p side,

Rather than apply the golden rule to second order, we calculate the above processes by first determining the eigenfunctions of H_0+H_1 to first order in H_1 and then use the golden rule to first order in the electron-phonon interaction to calculate the current. This corresponds to the method used previously for phonon-assisted tunneling in superconductors.[17] We therefore proceed to calculate the admixture of a $\Gamma_{2'}$ tail in the n region to the $\Gamma_{25'}$ wave function in the p region using first-order perturbation theory. From (16) and (46) and defining

$$\Delta_0=\Delta_\Gamma-Eel=\Delta_\Gamma-\Delta_L-\zeta_h-\zeta_e+e\mathcal{V}, \tag{56}$$

$$B=\tfrac{1}{2}(m_r\Delta_\Gamma/\hbar^2+\mathbf{k}_{\perp v}^2)^{1/2}, \tag{57}$$

$$\gamma=2B[l-(eE)^{-1}(\hbar^2\mathbf{k}_{\perp v}^2/6m_r+\hbar^2k_{\parallel v}^2/2m_v+\tfrac{1}{6}\Delta_\Gamma)], \tag{58}$$

we obtain

$$\beta_{\text{tail}}(\rho)=\frac{L}{2\pi}\int_0^\infty\frac{M(\mathbf{k}_v,k_{\parallel\Gamma c})\beta_{\Gamma c}(\rho)dk_{\parallel\Gamma c}}{\Delta_0+\frac{1}{2}\hbar^2[k_{\parallel\Gamma c}^2/m_{\Gamma c}+k_\perp^2/m_r+k_{\parallel v}^2/m_v]}=-\tfrac{1}{2}i\hbar^2$$
$$\times V^{-1/2}\exp[\tfrac{1}{3}i\hbar^2k_{\parallel v}^3/m_veE][\Delta_\Gamma m_r/(\Delta_\Gamma m_r+\hbar^2k_\perp^2)]^{1/2}e^{-\gamma}(-k_{\parallel v}/m_{\Gamma c}m_v)^{1/2}$$
$$\times\int_0^\infty\frac{\sin(-k_{\parallel\Gamma c}\rho+\frac{1}{3}\hbar^2k_{\parallel\Gamma c}^3/m_{\Gamma c}eE+\pi/4)(k_{\parallel\Gamma c})^{1/2}}{\Delta_0+\frac{1}{2}\hbar^2[k_{\parallel\Gamma c}^2/m_{\Gamma c}+\mathbf{k}_\perp^2/m_r+k_{\parallel v}^2/m_v]}\exp(\hbar^2k_{\parallel\Gamma c}^2B/m_{\Gamma c}eE)dk_{\parallel\Gamma c}, \tag{59}$$

in the region $\rho<0$. Dropping the unimportant phase factors which will cancel out when the electron-phonon matrix element is squared and changing the lower limit of integration to $-\infty$,[18] we obtain

$$\beta_{\text{tail}}(\rho)=\frac{\hbar^2V^{-1/2}}{4}\left(\frac{\Delta_\Gamma m_r}{\Delta_\Gamma m_r+\hbar^2k_\perp^2}\right)^{1/2}(k_{\parallel v}/m_{\Gamma c}m_v)^{1/2}$$
$$\times e^{-\gamma}\int_{-\infty}^\infty\frac{(k_{\parallel\Gamma c})^{1/2}\exp[ik_{\parallel\Gamma c}\rho-\frac{1}{3}i\hbar^2k_{\parallel\Gamma c}^3/m_{\Gamma c}eE+\hbar^2k_{\parallel\Gamma c}^2B/m_{\Gamma c}eE]}{\Delta_0+\frac{1}{2}\hbar^2[k_{\parallel\Gamma c}^2/m_{\Gamma c}+\mathbf{k}_\perp^2/m_r+k_{\parallel v}^2/m_v]}dk_{\parallel\Gamma c}. \tag{60}$$

In the lowest order the exponential alone determines the points of stationary phase at

$$k_{\parallel s}=-iB\pm i(B^2-m_{\Gamma c}eE\rho/\hbar^2)^{1/2}. \tag{61}$$

In Fig. 2 we show how the path of integration may be distorted to lie along the path of steepest descents through the point of stationary phase on the negative imaginary axis. The contribution to the integral from the saddle point is negligible compared with the contribution from the pole[19] at

$$k_{\parallel p}=-iG=-im_{\Gamma c}^{1/2}(2\Delta_0\hbar^{-2}+k_{\parallel v}^2/m_v+\mathbf{k}_{\perp v}^2/m_r)^{1/2}=-i(2m_{\Gamma c})^{1/2}\hbar^{-1}[\Delta_0+\mathcal{E}_v^0+(m_v/m_r-1)\mathcal{E}_{\perp v}^0]^{1/2}, \tag{62}$$

which by the method of residues gives

$$\beta_{\text{tail}}(\rho)=\tfrac{1}{2}m_{\Gamma c}V^{-1/2}\pi[\Delta_\Gamma m_r/(\Delta_\Gamma m_r+\hbar^2\mathbf{k}_{\perp v}^2)]^{1/2}(k_{\parallel v}/m_{\Gamma c}m_v)^{1/2}G^{-1/2}e^{-\gamma}e^{\hbar^2G^3/3m_{\Gamma c}eE}e^{-\hbar^2G^2B/m_{\Gamma c}eE}e^{G\rho}, \quad \rho<0. \tag{63}$$

[17] L. Kleinman, Phys. Rev. **132**, 2484 (1963).

[18] $\int_0^\infty x^{1/2}\sin(x+\frac{1}{4}\pi)dx=2^{-1/2}\int_0^\infty x^{1/2}(\sin x+\cos x)dx=2^{-1/2}\left\{\frac{1}{1+i}\int_{-\infty}^\infty x^{1/2}\sin x\,dx+\frac{1}{1-i}\int_{-\infty}^\infty x^{1/2}\cos x\,dx\right\}=2^{-3/2}(1+i)\int_{-\infty}^\infty x^{1/2}e^{-ix}dx.$

[19] For sufficiently large negative values of ρ the saddle-point contribution exceeds that of the pole but both terms are then negligible.

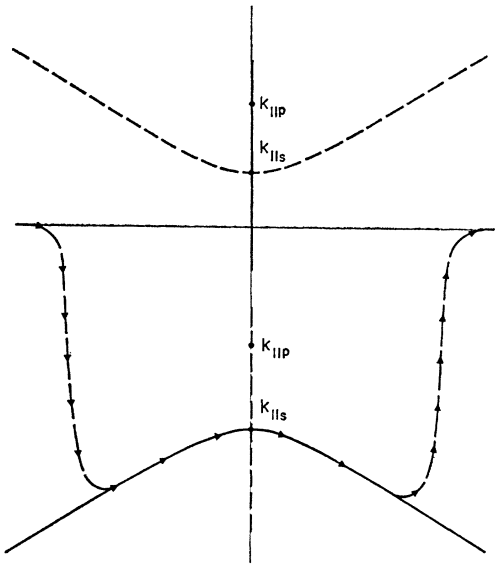

FIG. 2. Path of integration in complex k_{ll} plane. The solid lines are paths of steepest descent through the saddle points $k_{ll_s}=-iB\pm i(B^2-m_{\Gamma c}eE\rho/\hbar^2)^{1/2}$ (note ρ is negative). The short dashed lines are paths of steepest ascent. There are two poles at $k_{ll_p}=\pm i(2m_{\Gamma c})^{1/2}\hbar^{-1}[\Delta_0+\mathcal{E}_v{}^0+(m_v/m_r-1)\mathcal{E}_{v\perp}{}^0]^{1/2}$.

The LA phonon-assisted current is given by the first-order golden rule [Eq. (48)] but replacing the matrix element there with

$$\langle\psi_{Lc}(\mathbf{k}_{Lc})|H_{\text{LA el ph}}|\psi_v(\mathbf{k}_v)\rangle\approx M_{\text{LA}}V_{\text{ph}}{}^{-1/2}\langle V_n{}^{-1/2}|\beta_{\text{tail}}(\rho)\rangle. \tag{64}$$

We take $V_{\text{ph}}\approx\mathcal{A}G^{-1}$, the volume over which $\beta_{\text{tail}}(\rho)$ is large, integrate $\beta_{\text{tail}}(\rho)$ between 0 and $-\infty$, use $k_{ll_v}d^3k=(m_v{}^2/\hbar^4)d\mathcal{E}_v{}^0d\mathcal{E}_{\perp v}{}^0d\theta$ and $d^3k_{Lc}=[m_{Lc}{}^t(m_{Lc}{}^l)^{1/2}/\hbar^3]\mathcal{E}_{Lc}{}^{0\,1/2}d\mathcal{E}_{Lc}{}^0\sin\theta d\theta d\phi$ where $m_{Lc}{}^l$ and $m_{Lc}{}^t$ are the longitudinal and transverse L_1 effective masses, to write

$$J=\frac{eM_{\text{LA}}{}^2\mathcal{A}m_vm_{\Gamma c}m_{Lc}{}^t(m_{Lc}{}^l)^{1/2}}{4\sqrt{2}(2\pi)^2\hbar^8}\int\left(\frac{\Delta_\Gamma m_r}{\Delta_\Gamma m_r+\hbar^2k_{\perp v}{}^2}\right)(f_{Lc}-f_v)$$

$$\times\delta(\mathcal{E}_{Lc}-\mathcal{E}_v\mp\hbar\omega)\exp[2\hbar^2G^3/3m_{\Gamma c}eE-2\hbar^2G^2B/m_{\Gamma c}eE-2\gamma]G^{-2}\mathcal{E}_{Lc}{}^{0\,1/2}d\mathcal{E}_{Lc}{}^0d\mathcal{E}_v{}^0d\mathcal{E}_{\perp v}{}^0. \tag{65}$$

The integration over $\mathcal{E}_{Lc}{}^0$ to eliminate the δ function is trivial. We integrate $\mathcal{E}_{\perp v}{}^0$ between the limits 0 and $\mathcal{E}_v{}^0$. Because the integrand is smaller by a factor e^{-6} at the upper limit we may ignore $\mathcal{E}_{\perp v}{}^0$ (compared with $\mathcal{E}_v{}^0$) where it appears outside the exponential. The G^3 term is the least important one in the exponential so we do not make too serious an error when we approximate it by $(2m_{\Gamma c})^{1/2}\hbar^{-1}(\Delta_0+\mathcal{E}_v{}^0)^{1/2}G^2$. Note that with the parameters listed in Table II, Δ_0 is negative for negative or small positive voltage but $\Delta_0+\mathcal{E}_v{}^0$ is always positive. Thus we obtain

$$J=\frac{eM_{\text{LA}}{}^2\mathcal{A}m_vm_{Lc}{}^t(m_{Lc}{}^l)^{1/2}}{64\sqrt{2}\pi^2\hbar^5}\int_0^\infty\exp\left\{-\frac{2}{eE\hbar}[\tfrac{5}{6}m_r{}^{1/2}\Delta_\Gamma{}^{3/2}-\tfrac{2}{3}(2m_{\Gamma c})^{1/2}(\Delta_0+\mathcal{E}_v{}^0)^{3/2}]\right\}eE[(m_r\Delta_\Gamma)^{1/2}(\tfrac{5}{6}+\tfrac{2}{3}m_v/m_r)$$

$$-2(2m_{\Gamma c})^{1/2}(\Delta_0+\mathcal{E}_v{}^0)^{1/2}(m_v/m_r-1)]^{-1}\left[1-\exp\left\{-\frac{2}{\hbar eE}[(m_r\Delta_\Gamma)^{1/2}(\tfrac{5}{6}+\tfrac{2}{3}m_v/m_r)-2(2m_{\Gamma c})^{1/2}\right.\right.$$

$$\left.\left.\times(\Delta_0+\mathcal{E}_v{}^0)^{1/2}(m_v/m_r-1)]\mathcal{E}_v{}^0\right\}\right](\zeta_e+\zeta_h-e\mathcal{U}\pm\hbar\omega-\mathcal{E}_v{}^0)^{1/2}(\Delta_0+\mathcal{E}_v{}^0)^{-1}(f_{Lc}-f_v)d\mathcal{E}_v{}^0, \tag{66}$$

where we have used

$$\mathcal{E}_v=Eel-\Delta_L-\mathcal{E}_v{}^0=\zeta_h+\zeta_e-e\mathcal{U}-\mathcal{E}_v{}^0.$$

The Fermi functions may be replaced by step functions giving the limits of integration shown in Table I.

In calculating (66) we have not considered β_{tail} in the region $\rho>0$. If in Eq. (59) we use Eq. (12), $\beta_{\Gamma c}(\rho)=N_cA[\alpha_c(1-\rho/\rho_c)]$, we find ourselves unable to evaluate the integral exactly. β_{tail} represents the n-side $\Gamma_{2'}$ character admixed into the p-side $\Gamma_{25'}$ wave function by the interband term in the Hamiltonian. We have shown it falls off exponentially for $\rho<0$ because of the exponential falloff of $\Gamma_{25'}$ itself. For $\rho>0$, providing the major contributions to β_{tail} come from the bottom of the Γ_2' band, we would also expect β_{tail} to fall off exponentially because the n-side Γ_2' functions fall off exponentially for $\rho>0$. We have evaluated the integral (59), substituting the asymptotic expression for $A[\alpha_c(1-\rho/\rho_c)]$ valid for $(\hbar^2/2m_{\Gamma c}eE)^{2/3}k_{ll\Gamma c}{}^2-(\hbar^2/2m_{\Gamma c}eE)^{-1/3}\rho\ll0$. This expression is also valid everywhere in the complex $k_{ll\Gamma c}$

TABLE II. Values of quantities defined in text.

$m_{\Gamma c}=0.034m$	$\Delta_\Gamma=0.803$ eV
$m_v=0.044m$	$\Delta_L=0.66$ eV
$m_r=0.0192m$	$\Delta_{LL}=2.1$ eV
$m_{Lc}{}^t=0.082m$	$\hbar\omega_{LA}=0.028$ eV
$m_{Lc}{}^l=1.58m$	$\hbar\omega_{TA}=0.0076$ eV
$(m_{Lc}{}^{-1})_\perp=7.108m^{-1}$	$n^*=5.04\times10^{18}$ cm^{-3}
$(m_{Lc}{}^{-1})_{II}=8.341m^{-1}$	$\kappa=16$
$m_{Lr}=0.0322m$	$E=(1.62-0.98\mathcal{U})10^3$ esu ($\mathcal{U}$ in volts)
$\zeta_e=0.020$ eV	$M_{TA}{}^2=M_{LA}{}^2=4.3\times10^{-49}$ erg cm^3
$\zeta_h=0.15$ eV	$\mathcal{A}=0.002$ cm^2
$d\Delta_\Gamma/dP=12\times10^{-12}$ eV cm^2/dyn	$d\zeta_e/dP=-2.92\times10^{-14}$ eV cm^2/dyn
$d\Delta_L/dP=5\times10^{-12}$ eV cm^2/dyn	$d\zeta_h/dP=1.17\times10^{-13}$ eV cm^2/dyn
$d\Delta_{LL}/dP=7.5\times10^{-12}$ eV cm^2/dyn	$V^{-1}dV/dP=-1.38\times10^{-12}$ cm^2/dyn

plane that $|(\hbar^2/2m_{\Gamma c}eE)^{2/3}k_{II\Gamma c}{}^2-(\hbar^2/2m_{\Gamma c}eE)^{-1/3}\rho|\gg0$ except along the real axis. However, for $k_{II\Gamma c}$ very large and real, $A[\alpha_c(1-\rho/\rho_c)]$ oscillates like $\sin k_{II\Gamma c}{}^3$ and thus does not contribute to the integral. We find saddle points and poles (in regions where the asymptotic expression is valid) leading to the same exponential falloff as for the $\rho<0$ case. We therefore take the total LA phonon-assisted current to be twice that given by Eq. (66). Although we believe the preceding arguments to be valid, we cannot claim to have proven beyond any doubt that the contribution to the phonon-assisted tunneling current from $\rho>0$ is not much greater than from $\rho<0$. Since the main purpose of this paper is to demonstrate that the second-order process yields a current at least three orders of magnitude greater than the first-order process, such an error would only serve to strengthen our argument.

VII. COMPARISON WITH EXPERIMENT

We integrate Eq. (55) between the limits shown in Table I for positive and negative voltages such that $|e\mathcal{U}-\hbar\omega|<\zeta_e$, to obtain

$$J_{TA}{}^\pm=Q^\mp\{(e\mathcal{U}\mp\hbar\omega)(1+e^{-R^\mp(\zeta_h+\zeta_e-e\mathcal{U}\pm\hbar\omega)})+(R^\mp)^{-1}[e^{-R^\mp\zeta_e}-e^{-R^\mp(\zeta_e-e\mathcal{U}\pm\hbar\omega)}+e^{-R^\mp\zeta_h}-e^{-R^\mp(\zeta_h-e\mathcal{U}\pm\hbar\omega)}]\}, \quad (67)$$

where

$$Q^\mp=\sqrt{2}\,\mathcal{A}eM_{TA}{}^2(eE)^2m_v\times\exp[-\tfrac{4}{3}(2m_{Lr})^{1/2}(eE\hbar)^{-1}(\Delta_L\mp\hbar\omega)^{3/2}]/16\pi^2m_{Lr}{}^{1/2}\hbar^4(m_{Lc}{}^{-1})_\perp(\Delta_L\mp\hbar\omega)^{5/2}, \quad (68)$$

$$R^\mp=2(2m_{Lr})^{1/2}(\Delta_L\mp\hbar\omega)^{1/2}/eE\hbar. \quad (69)$$

We may evaluate the integral (66) for small voltages by writing $\mathcal{E}_v{}^0=\zeta_h+\chi$ and treating χ as small (χ is between the limits 0 and $-e\mathcal{U}\pm\hbar\omega$). Expanding the first exponential to first order in χ and the second one to first order in $\mathcal{E}_v{}^0$ and integrating (66) we obtain

$$J_{LA}=\mathcal{S}\{[\zeta_e{}^{3/2}-(\zeta_e-e\mathcal{U}\pm\hbar\omega)^{3/2}]+\tfrac{1}{5}[\zeta_e{}^{3/2}(2\zeta_e-5e\mathcal{U}\pm5\hbar\omega)-2(\zeta_e-e\mathcal{U}\pm\hbar\omega)^{5/2}]\times[2(2m_{\Gamma c})^{1/2}(\Delta_0+\zeta_h)^{1/2}/eE\hbar+\Delta_0/\zeta_h(\Delta_0+\zeta_h)]\}, \quad (70)$$

where

$$\mathcal{S}=eM_{LA}{}^2\mathcal{A}m_vm_{Lc}{}^tm_{Lc}{}^{l\,1/2}\exp\{-(2/eE\hbar)\times[\tfrac{5}{6}m_r{}^{1/2}\Delta_\Gamma{}^{3/2}-\tfrac{2}{3}(2m_{\Gamma c})^{1/2}(\Delta_0+\zeta_h)^{3/2}]\}\times\zeta_h/48\sqrt{2}\pi^2\hbar^6(\Delta_0+\zeta_h). \quad (71)$$

In both (67) and (70) a sum over the four L_1 valleys is implied. We calculate the current for a (1,0,0) junction where all the valleys are equivalent. In Table II we list numerical values for all the parameters in (67) and (70) using[16]

$$E=[2\pi n^*(\Delta_L+\zeta_e+\zeta_h-e\mathcal{U})/\kappa]^{1/2}, \quad (72)$$

where $n^*=np/(n+p)$ is the reduced doping constant and κ is the dielectric constant. It should be pointed out that our J_{TA} differs from Kane's[4] by a dimensionless prefactor $[eEh/m_vm_{Lc}{}^l]^{1/2}[2m_{Lr}/\Delta_L]^{3/4}[2/m_{Lc}{}^t(m_{Lc}{}^{-1})_\perp]=0.66$. In Fig. 3 we plot the calculated currents. Comparison with Fig. 2 of Ref. 16, shows that J_{LA} is in remarkable agreement[20] with experiment but J_{TA} is too

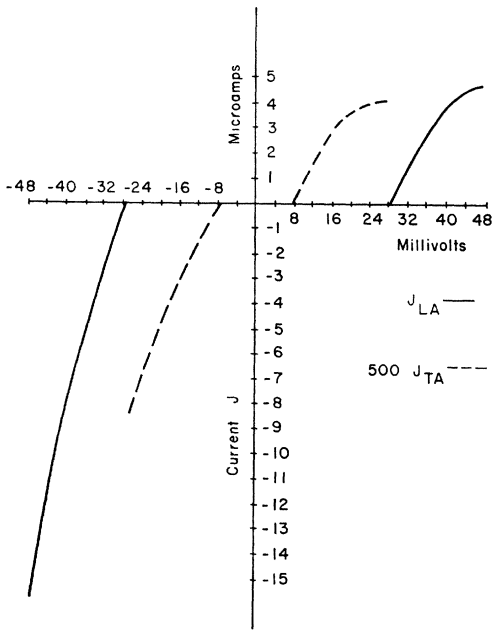

FIG. 3. Plot of J_{LA}, the second-order longitudinal phonon-assisted tunneling current, and 500 J_{TA}, the first-order transverse phonon-assisted tunneling current, versus voltage.

[20] Because of the fixed average electric field, the effective mass, and the two band approximations, one should expect the exponent in (71) to be in error by several percent leading to factors of 2 or 3 in the current. Therefore the remarkable agreement between theory and experiment is to that extent fortuitous.

small by over two orders of magnitude. Actually in Fig. 2 Fritzsche and Tiemann[16] plot the characteristics of a (1,1,0) junction but they state that these differ from their (1,0,0) junction by less than 10%. Note that our second-order process [Eqs. (70) and (71)] is independent of junction orientation but that the first-order process [Eqs. (67), (68), and (69)] depends exponentially through m_{Lr} on the junction orientation. Thus for a (1,1,0) junction J_{TA} is a factor of four smaller than shown in Fig. 3 differing from experiment by almost three orders of magnitude. Therefore even though the first-order phonon-assisted tunneling mechanism leads to approximately correct values for the pressure coefficients[8] it cannot be responsible for the TA current. This accounts for the failure of Nathan[21] to obtain from experimental data the correct prefactor A in Kane's formula $J=A\mathcal{V}e^{-\lambda(\mathcal{V})}$.

We calculate the pressure coefficients for the LA phonon-assisted current given by Eq. (70), assuming m_v and $m_{\Gamma c}$ are directly proportional to Δ_Γ, $m_{Lc}{}^t$ is directly proportional to Δ_{LL}, the $L_1-L_{3'}$ gap, and $m_{Lc}{}^l$ is pressure independent. This leads to

$$d\zeta_e/dP=-\tfrac{2}{3}\zeta_e[V^{-1}dV/dP+\Delta_{LL}{}^{-1}d\Delta_{LL}/dP]$$

and

$$d\zeta_h/dP=-\zeta_h[\tfrac{2}{3}V^{-1}dV/dP+(m_v/m)^{3/2}\Delta_\Gamma{}^{-1}d\Delta_\Gamma/dP],$$

where the factor $(m_v/m)^{3/2}$ accounts for the fact that it is the heavy holes which really determine ζ_h. Using the values for the pressure dependence of the various quantities listed in Table II and neglecting the pressure dependence of the the electron-phonon matrix element $MV^{-1/2}$ (which should be of the order of $V^{-1}dV/dP$), we compare $\pi_{LA}{}^+$ and $\pi_{LA}{}^-$ with the experimental values in Table III. Considering the simple pressure dependence assumed for the effective masses, the agreement is quite satisfactory both for $\pi_{LA}{}^++\pi_{LA}{}^-$ and $\pi_{LA}{}^+-\pi_{LA}{}^-$. Note that for the first-order phonon-assisted mechanism given by Eqs. (67) and (68) most of the forward-reverse asymmetry is due to the $(\Delta_L\mp\hbar\omega)^{3/2}$ term in the exponential. For the second-order mechanism, however, there is no exponential $\hbar\omega$ dependence because energy is not conserved between the initial and intermediate states. The large forward-reverse asymmetry is rather caused mainly by the voltage dependence of the energy denominator $\Delta_0+\zeta_h=\Delta_\Gamma-\Delta_L-\zeta_e+e\mathcal{V}$ in Eqs. (70) and (71).

The TA phonon-assisted current may be understood as caused by the same second-order process as the LA-assisted current if we consider the symmetry breaking due to the $\mathbf{k}\cdot\mathbf{p}$ perturbation. The $\Gamma_{2'}$ tail of Eq. (63) falls off with a characteristic wave number $G\approx 3.44\times10^6$ cm^{-1}. Now the $\Gamma_{2'}$ tail has a fraction χ_Γ of $\Gamma_{25'}$ character mixed into it given by

$$\chi_\Gamma\approx(\tfrac{2}{3})^{1/2}(GP_\Gamma)/\Delta_\Gamma\approx0.342, \qquad (73)$$

[21] M. I. Nathan, J. Appl. Phys. 33, 1460 (1962).

TABLE III. Comparison of experimental pressure coefficients $\pi=J^{-1}dJ/dP$ with theoretical ones in units of cm^2/dyn. The π_{LA}'s were calculated at applied voltages of ±0.038 and ±0.032, the π_{TA}'s at ±0.0156. The two contributions to π_{TA} come from the pressure dependence of Eq. (70) and the symmetry-breaking factor.

	Experiment	Theory
$\pi_{LA}{}^+$	-2.07×10^{-10}	-2.61, -2.62×10^{-10}
$\pi_{LA}{}^-$	-2.46×10^{-10}	-3.16, -3.13×10^{-10}
$\pi_{TA}{}^+$	-1.47×10^{-10}	$-2.76+0.38=-2.38\times10^{-10}$
$\pi_{TA}{}^-$	-1.56×10^{-10}	$-2.94+0.47=-2.47\times10^{-10}$

where we have evaluated P_Γ from Eq. (35). Since the transverse component of wave vector is conserved in direct tunneling, the $\Gamma_{2'}$ tail has a $\mathbf{k}_\perp$ which may be as large as the Fermi momentum of the $\Gamma_{25'}$ holes. However, we see from Eqs. (63), (62), and (57) that only when $\mathbf{k}_\perp\sim0$ is the $\Gamma_{2'}$ tail large. Thus Eq. (73) represents the total symmetry breaking for $\Gamma_{2'}$. In addition, the final L_1 state has a fraction $\chi_L\approx k_{Ft}P_L/\Delta_{LL}\approx0.113$ of $L_{3'}$ character mixed into it where $P_L=\hbar(\Delta_{LL}/2m_{Lc}{}^t)^{1/2}$ and $k_{Ft}=(4\zeta_e m_{Lc}{}^t/3\hbar^2)^{1/2}$ is the average transverse (to the axis of the constant energy ellipsoid) component of the electron Fermi wave vector. Furthermore using a first- and second-neighbor force-constant model we are able to estimate the fraction of LA character mixed into the TA phonon of wave vector $(\pi/a-G,\pi/a,\pi/a)$ and find $\chi_{ph}\approx0.017$. These three contributions come in with arbitrary phase so that the cross terms cancel out and (if we assume $M_{TA}=M_{LA}$) the TA-assisted current at a given $(e\mathcal{V}-\hbar\omega_{TA})$ is approximately equal to $2(\chi_\Gamma{}^2+\chi_L{}^2+\chi_{ph}{}^2)$ times the LA current at the same value of $(e\mathcal{V}-\hbar\omega_{LA})$. The factor 2 arises from the two TA phonon branches. Thus we find $J_{TA}(e\mathcal{V})\approx0.26\,J_{LA}(e\mathcal{V}+\hbar\omega_{LA}-\hbar\omega_{TA})$ in excellent agreement with experiment.[16]

The pressure dependence of the TA current has two terms. The first is from the pressure dependence of Eq. (70) and is the same as one gets for LA phonons but has a smaller forward-reverse asymmetry because of the smaller voltage required to get the TA current. The second is just $2(\chi_\Gamma d\chi_\Gamma/dP\times\chi_L d\chi_L/dP+\chi_{ph}d\chi_{ph}/dP)/(\chi_\Gamma{}^2+\chi_L{}^2+\chi_{ph}{}^2)$. These contributions are listed in Table III. The cancellation between these two terms accounts for more than half of the experimental value of $(\pi_{LA}{}^++\pi_{LA}{}^-)-(\pi_{TA}{}^++\pi_{TA}{}^-)$.

In summary we have shown that the second-order phonon-assisted tunneling mechanism yields a current about 1000 times as large as the direct phonon-assisted mechanism and accounts for both the LA and TA currents. The reasons for the dominance of the second-order mechanism are twofold. When a phonon scatters a left-hand electron into a right-hand state, if the interaction takes place in a region where the right-hand state has large amplitude, then the left-hand state will have small amplitude and vice versa. On the other hand the

interband tunneling operator is nonlocal [Eq. (40)] and therefore is not quite so affected by the fact that where one wave function is large, the other is small. The second reason for the dominance of the indirect mechanism is of course that there is a nearby band of intermediate states to be mixed in by the nonlocal operator.

The author would like to thank Professor H. Fritzsche for informative discussions.

PHYSICAL REVIEW VOLUME 140, NUMBER 2A 18 OCTOBER 1965

Effective Hyperfine Fields at the Nuclei of Os and Pt Dissolved in Fe*

JAMES C. HO AND NORMAN E. PHILLIPS†
Inorganic Materials Division of the Lawrence Radiation Laboratory and Department of Chemistry, University of California, Berkeley, California

(Received 17 May 1965)

The heat capacities of two alloys containing, respectively, 0.75 at.% Os and 3.21 at.% Pt dissolved in Fe have been measured from 0.08 to 1.15°K. From the coefficients of the T^{-2} terms, the hyperfine fields at the nuclei were found to be 1400 kOe for Os and 1390 kOe for Pt.

IN recent years a number of experimental techniques have been used to measure the product of the nuclear magnetic-dipole moment μ and the effective magnetic hyperfine field H_e for a dilute impurity in a ferromagnetic metal. The results are of interest because they give information about nuclear moments and also because a systematic study of H_e values may contribute to a better understanding of ferromagnetism. The calorimetric determination of μH_e is based on measurement of the contribution to the hyperfine heat capacity associated with the impurity nuclei. For 1 mole of sample, and at temperatures $T \gg \mu H_e/k$ (k is Boltzmann's constant), this contribution C is given by

$$\frac{C}{fR}=\frac{1}{3}\left\langle\frac{I+1}{I}\mu^2\right\rangle_{\rm av}\left(\frac{H_e}{kT}\right)^2 -\frac{1}{30}\left\langle\frac{(I+1)(2I^2+2I+1)}{I^3}\mu^4\right\rangle_{\rm av}\left(\frac{H_e}{kT}\right)^4+\cdots, \quad (1)$$

where f is the atomic fraction of impurity, R is the gas constant, I is the nuclear spin, and the average is taken over the isotopic composition of the impurity. The calorimetric method is limited to alloys for which the contribution from nuclei of the impurity is large relative to that from nuclei of the host metal, but it is a useful complement to the methods based on nuclear orientation and the Mössbauer effect, each of which can also be used only in certain cases. Furthermore, Eq. (1) involves μ for the nuclear ground state, which is usually known, whereas the nuclear orientation method—and in some cases the Mössbauer method—give the product of H_e and μ for an excited state. A combination of two experiments may therefore give both H_e and the excited-state μ. We present here a calorimetric determination of H_e for Os and Pt dissolved in Fe.

An alloy of iron with 3.21 at.% Pt was prepared by melting 99.999% iron sponge and 99.9% Pt foil chips in a helium atmosphere, and was homogenized by annealing for 20 h at 1300°C. A sample containing 0.75 at.% Os in iron of the same purity was supplied by Johnson, Matthey and Company, Ltd. The heat-capacity measurements were carried out in the temperature range 0.08 to 1.15°K with an apparatus previously described by O'Neal and Phillips.[1]

The experimental data were analyzed by plotting CT^2 versus T^3, as shown in Figs. 1 and 2. The straight-line regions of these plots gave the T^{-2} and T terms in the heat capacities,

$$C(\text{mJg}^{-1}\,\text{deg}^{-1})=8.36\times10^{-2}T+1.12\times10^{-4}T^{-2} \quad (2)$$

for 0.75 at.% Os in Fe, and

$$C(\text{mJg}^{-1}\,\text{deg}^{-1})=8.25\times10^{-2}T+1.40\times10^{-3}T^{-2} \quad (3)$$

for 3.21 at.% Pt in Fe. The observed T^{-2} terms were corrected by subtracting the contribution expected for the Fe nuclei in pure iron (the corrections were 3.3% and 0.25% for the Os and Pt samples, respectively) and were then used to calculate H_e values by comparison with Eq. (1). The comparison was based on the following data[2] for the isotopic abundances, spins, and nuclear moments: 1.64% Os^{187} with $I=\frac{1}{2}$, $=0.12$ nm; 16.1% Os^{189} with $I=\frac{3}{2}$, $\mu=0.6507$ nm; 33.8% Pt^{195} with $I=\frac{1}{2}$, $\mu=0.6004$ nm. The resulting values of H_e—1400 kOe for Os and 1390 kOe for Pt—were used to calculate the expected T^{-4} terms in the heat capacity. (The contributions of the Fe nuclei to the T^{-4} terms are completely negligible.) On this basis, the hyperfine heat

* Work supported by the U. S. Atomic Energy Commission.
† Alfred P. Sloan Research Fellow 1962–64. We are grateful to the Alfred P. Sloan Foundation for this support during the period in which the experiments were carried out.

[1] H. R. O'Neal and N. E. Phillips, Phys. Rev. **137**, A748 (1965).
[2] D. Strominger, I. M. Hollander, and G. T. Seaborg, Rev. Mod. Phys. **30**, 585 (1958).